THE JOURNAL OF BIOLOGICAL CHEMISTRY VOL. 288, NO. 23, pp. 16715–16725, June 7, 2013

WDR26 Functions as a Scaffolding Protein to Promote Gβγ-mediated Phospholipase C β2 (PLCβ2) Activation in Leukocytes*

Received for publication, February 17, 2013, and in revised form, April 9, 2013 Published, JBC Papers in Press, April 26, 2013, DOI 10.1074/jbc.M113.462564

Zhizeng Sun[‡], **Alan V. Smrcka**[§], **and Songhai Chen**[‡¶1]

From the Departments of [‡]*Pharmacology and* [¶]*Internal Medicine, Roy J. and Lucille A. Carver College of Medicine, University of Iowa, Iowa City, Iowa 52242 and the* [§]*Department of Pharmacology and Physiology, University of Rochester School of Medicine and Dentistry, Rochester, New York 14642*

Background: It remains unclear how Gβγ regulates diverse effectors in cells.
Results: WDR26 exists in oligomers. It simultaneously binds both Gβγ and PLCβ2 to enhance PLCβ2 membrane translocation and activation by Gβγ in leukocytes.
Conclusion: WDR26 functions as a scaffolding protein to promote Gβγ-mediated PLCβ2 activation.
Significance: These findings uncover a novel mechanism of regulating Gβγ signaling through a scaffolding protein.

We have recently identified WDR26 as a novel WD40 repeat protein that binds Gβγ and promotes Gβγ signaling during leukocyte migration. Here, we have determined the mechanism by which WDR26 enhances Gβγ-mediated phospholipase C β2 (PLCβ2) activation in leukocytes. We show that WDR26 not only directly bound Gβγ but also PLCβ2. The binding sites of WDR26 and PLCβ2 on $G\beta_1\gamma_2$ were overlapping but not identical. WDR26 used the same domains for binding Gβγ and PLCβ but still formed a signaling complex with Gβγ and PLCβ2 probably due to the fact that WDR26 formed a higher order oligomer through its Lis homology and C-terminal to LisH (LisH-CTLH) and WD40 domains. Additional studies indicated that the formation of higher order oligomers was required for WDR26 to promote PLCβ2 interaction with and activation by Gβγ. Moreover, WDR26 was required for PLCβ2 translocation from the cytosol to the membrane in polarized leukocytes, and the translocation of PLCβ2 was sufficient to cause partial activation of PLCβ2. Collectively, our data indicate that WDR26 functions as a scaffolding protein to promote PLCβ2 membrane translocation and interaction with Gβγ, thereby enhancing PLCβ2 activation in leukocytes. These findings have identified a novel mechanism of regulating Gβγ signaling through a scaffolding protein.

Heterotrimeric G proteins are composed of Gα and Gβγ subunits. They transduce diverse extracellular signals from G protein-coupled receptors to mediate many important cellular functions (1). The Gβγ subunits play a central role in G protein signaling. They tether Gα subunits to the membrane and regulate the duration of their activation (2). In addition, they directly interact with and modulate the activity of a long list of proteins including receptors, ion channels, and enzymes such as PLC,[2] phosphoinositide 3-kinases (PI3Ks), and G protein-coupled receptor kinase 2. Through these downstream targets, Gβγ regulates diverse functions including immune and tumor cell migration (3–5), yeast cell mating (6), and heart rate (7).

Gβ is a WD40-containing protein that possesses no enzymatic activities. Dimerization with prenylated Gγ subunits renders its predominant localization in the plasma membranes (2). Depending on the cellular localization of its downstream effectors, Gβγ may regulate their activities by recruiting them to the plasma membrane, direct interaction-induced conformational change, or both (2). For example, Gβγ-mediated activation or inhibition of membrane-embedded potassium and calcium channels occurs by inducing an alteration in their conformation (8, 9). In the case of cytosolic proteins such as PLCβ2, PI3Kγ, or G protein-coupled receptor kinase 2 whose substrates are localized to the plasma membrane, activation of these proteins is mediated at least in part by recruitment to the plasma membrane by Gβγ (10–13). However, Gβγ may directly stimulate the catalytic activity of these proteins. For example, it has been shown that translocation is not necessary for Gβγ-mediated PLCβ2 activation *in vitro* (14, 15).

We have recently shown that Gβγ-mediated signal transduction in leukocytes depends on a novel Gβγ-interacting protein, WDR26 (16). WDR26 has been implicated in the regulation of the MAPK signaling pathway, neuronal and cardiomyoblast cell proliferation, and apoptosis (17–20). Down-regulation of WDR26 alleviated Gβγ-mediated PI3K and PLCβ activation and leukocyte chemotaxis, indicating that WDR26 is required for efficacious Gβγ signaling in leukocytes (16). Like Gβγ, WDR26 is a WD40 repeat-containing protein. Its C terminus is predicted to contain seven WD40 repeats, whereas its N terminus contains Lis homology (LisH) and C-terminal to LisH (CTLH) domains that are predicted to be involved in protein-

* This work was supported, in whole or in part, by National Institutes of Health Grant GM094255 (to S. C.).

[1] To whom correspondence should be addressed: Dept. of Pharmacology, Roy J. and Lucille A. Carver College of Medicine, University of Iowa, Bowen Science Bldg., Rm. 2-3452, 51 Newton Rd., Iowa City, IA 52242. Tel.: 319-384-4562; Fax: 319-335-8930; E-mail: songhai-chen@uiowa.edu.

[2] The abbreviations used are: PLC, phospholipase C; dHL60, differentiated HL60; IP, inositol phosphate; LisH, Lis homology; CTLH, C-terminal to LisH; fMLP, *N*-formylmethionine-leucine-phenylalanine; Ni-NTA, nickel-nitrilotriacetic acid; myr, myristoylated; MBP, maltose-binding protein.

protein interactions and protein dimerization. The binding of WDR26 to Gβγ involves the Gα contact surface of Gβγ that interacts with many known Gβγ effectors (16). It is not yet clear how WDR26 binding to Gβγ leads to enhanced Gβγ signaling.

Here, we provide evidence that WDR26 exists in a higher order oligomer and simultaneously binds both Gβγ and PLCβ2. It promotes PLCβ2 membrane translocation and functions as a scaffolding protein to bring PLCβ2 in close proximity to Gβγ for activation. Thus, our findings have uncovered a novel mechanism of regulating Gβγ signaling through a scaffolding protein.

EXPERIMENTAL PROCEDURES

Reagents—SDF1α was from PreproTech. *N*-formylmethionine-leucine-phenylalanine (fMLP), pertussis toxin, and fibronectin were from Sigma-Aldrich. Alexa Fluor 488- and 568-conjugated secondary antibodies, Alexa Fluor 568-conjugated phalloidin, CM-DiI, and Dynabeads protein G were from Invitrogen. Ni-NTA resin was from Thermo Scientific. Mouse anti-FLAG (M2) antibody was from Sigma-Aldrich. Rabbit anti-WDR26 antibody was from Bethyl Laboratories. Rabbit anti-Gβ (T20), rabbit anti-$G\alpha_i$, and rabbit anti-PLCβ2 antibodies were from Santa Cruz Biotechnology.

Cell Culture—Jurkat T cells stably expressing FLAG-WDR26 and the HL60 cell line (ATCC) were grown in RPMI 1640 medium (Invitrogen) containing 10% fetal bovine serum (FBS) as described previously (3, 16). HEK293 cells (ATCC) were maintained in DMEM (Invitrogen) supplemented with 10% FBS. Differentiation of HL60 cells into human neutrophil-like cells was induced by adding 1.3% DMSO to the growth medium and incubating for 7 days.

Transfection—Transient transfection of HEK293 cells was performed using Polyjet DNA *in vitro* transfection reagent (Signagen) as described (16). Transfection of differentiated HL60 (dHL60) cells (1×10^6) with siRNAs (0.2 nmol) was performed 5 days postdifferentiation using the Neon transfection system (Invitrogen) with 10-μl electroporation tips and electroporation parameters 1500 V/25 ms/one pulse (16).

DNA Constructs—The cDNAs for WDR26 and WDR26 deletion mutants WDR1–122, WDR1–231, WDR123–231, WDR232–661, and WDR123–661 were generated by PCR; some of them have been described previously (16). They were first cloned into the entry vector pENTR/SD/D-TOPO (Invitrogen) and then the destination vectors containing different tags including FLAG, myristoylated (myr)-FLAG, and maltose-binding protein (MBP) for expression in mammalian cells, Sf9 cells, and *Escherichia coli*, respectively, by using the Gateway cloning system (Invitrogen) as described. The myristoylation sequence was derived from the N-terminal amino acid sequence (amino acids 2–15) of the Src protein. The plasmids encoding rat PLCβ2 (pMT2-PLCβ2), HA-tagged human $G\beta_1$ (pcDNA3.1-HA-$G\beta_1$), and human $G\gamma_2$ have been described previously (16, 21). pcDNA3.1-FLAG-PLCβ2 and pcDNA3.1-myr-FLAG-PLCβ2 were constructed using the Gateway cloning system after PLCβ2 was cloned into the donor vector pDONR221 (Invitrogen).

Purification of WDR26 from E. coli—MBP, MBP-WDR26, and its mutants were expressed in *E. coli* BL21 cells and purified using amylose resin (New England Biolabs) (16, 21). MBP was removed from WDR26 by digestion with 3C protease at 4 °C overnight followed by gel filtration chromatography.

Purification of Proteins from Sf9 Cells—His_6-PLCβ2, $G\beta_1$/His-γ_2, FLAG-$G\beta_1$/His-γ_2, and $G\beta_1$W99A/His-γ_2 were purified from Sf9 cells infected with baculoviruses encoding the genes as described previously (22). FLAG-WDR26 was expressed in Sf9 cells and prepared as cell lysates as described (16).

Immunoprecipitation and Western Blotting Analysis—To co-immunoprecipitate FLAG-WDR26 with endogenous Gβγ and PLCβ2, Jurkat T cells were first serum-starved for 4–6 h and then stimulated with SDF1α (50 nM) for the indicated times. In some cases, cells were pretreated with pertussis toxin (0.2 μg/ml) overnight prior to stimulation by SDF1α. After SDF1α stimulation, 1 mM dithiobis(succinimidyl propionate) (Pierce) was added to cross-link the proteins for 40 min at room temperature followed by the addition of 50 mM Tris-HCl (pH 7.4) to quench the unreacted dithiobis(succinimidyl propionate). After washing twice with PBS (pH 7.4), cells were lysed in radioimmune precipitation assay buffer (50 mM Tris-HCl (pH 7.4), 150 mM NaCl, 1% Nonidet P-40, 0.1% SDS, 1% deoxycholate, 1 mM EDTA) containing protease inhibitors. Immunoprecipitation was performed as described previously (16). Protein complexes were resolved by SDS-PAGE and analyzed by Western blotting analysis using the Odyssey imaging system (LI-COR Biosciences).

To co-immunoprecipitate FLAG-WDR26 and its mutants with PLCβ2 following their expression in HEK293 cells, cell lysates were prepared from the transfected cells without dithiobis(succinimidyl propionate)-mediated protein cross-linking. FLAG-tagged proteins were immunoprecipitated as described above except that modified radioimmune precipitation assay buffer containing 1% Nonidet P-40 but no SDS and deoxycholate was used. Similar co-immunoprecipitation experiments were carried out to determine the interaction of WDR26 with its mutants.

Protein Binding Assays—To determine its binding to PLCβ2, 0.2 μM FLAG-WDR26 was first immunoprecipitated from the Sf9 cell lysates in radioimmune precipitation assay buffer using the anti-FLAG M2 antibody (Sigma) conjugated to Dynabeads protein G. The beads containing FLAG-WDR26 were washed extensively (five times) with radioimmune precipitation assay buffer to remove lipids and other proteins associated with WDR26 and beads and then incubated with increasing concentrations of PLCβ2 in buffer (50 mM Tris-HCl (pH 8.0), 150 mM NaCl, 1 mM EDTA, 0.2% Nonidet P-40) for 4 h at 4 °C. Protein complexes were precipitated using a magnetic stand and subjected to SDS-PAGE and immunoblot analysis.

To confirm the direct protein-protein interaction between WDR26 and PLCβ2, 0.2 μM purified His_6-PLCβ2 was incubated with increasing concentrations of purified WDR26 in buffer (20 mM HEPES (pH 8.0), 200 mM NaCl, 1 mM DTT, 5 mM imidazole, 0.2% Nonidet P-40) at 4 °C for 2 h. Protein complexes were precipitated by incubation with Ni-NTA resin at 4 °C for 2 h followed by washing three times with high salt buffer (20 mM HEPES (pH 8.0), 500 mM NaCl, 1 mM DTT, 0.2%

Nonidet P-40) and twice with binding buffer and then subjected to SDS-PAGE and immunoblot analysis.

To determine the effects of WDR26 and its mutants on the $G\beta_1\gamma_2$ and PLCβ2 interaction, 0.2 μM purified FLAG-$G\beta_1\gamma_2$ was incubated with 0.5 μM PLCβ2 and increasing concentrations of purified WDR26 (0–2 μM) or its mutant (0–1 μM). The protein complexes were then immunoprecipitated with the anti-FLAG M2 antibody conjugated to Dynabeads protein G as described above.

The binding of $G\beta_1\gamma_2$ and $G\beta_1$W99Aγ_2 to FLAG-WDR26 was determined as described previously (16). To determine the effects of M119, gallein, and M119B on $G\beta_1\gamma_2$ binding to FLAG-WDR26, M119, gallein, and M119B were first incubated with $G\beta_1\gamma_2$ for 1 h prior to the addition of FLAG-WDR26. To determine the effects of M119 and M119B on PLCβ2 binding to FLAG-WDR26, M119 and M119B were first incubated with precipitated FLAG-WDR26 for 1 h prior to the addition of PLCβ2.

Polarization of dHL60 Cells—Polarization of dHL60 cells to a uniform concentration of fMLP was performed in a Lab-Tek™ II 8-well chamber slide precoated with fibronectin (100 ng/ml). 5×10^4 dHL60 cells in 0.15 ml of Hanks' balanced salt solution (Invitrogen) supplemented with 1% glucose and 1% human serum albumin were seeded onto each well and incubated at 37 °C for 10 min. After washing twice with Hanks' balanced salt solution to remove unattached cells, cells were stimulated with buffer or 100 nM fMLP for 3 min at room temperature and then fixed with 4% paraformaldehyde and 0.05% glutaraldehyde (Sigma) for 10 min.

Immunofluorescence Staining—To stain for PLCβ2 and WDR26 in polarized dHL60 cells or HEK293 cells transiently transfected with PLCβ2, myr-PLCβ2, FLAG-WDR26, myr-FLAG-WDR26, or myr-FLAG-WDR26 plus PLCβ2, cells fixed with 4% paraformaldehyde were permeabilized by 0.5% Triton X-100 and then incubated with rabbit anti-PLCβ2 antibody (1:50 dilution), anti-WDR26 (1:250 dilution), or mouse anti-FLAG antibody (1:500 dilution) for 2 h at room temperature followed by incubation with an Alexa Fluor 488- or 568-conjugated anti-rabbit secondary antibody (1:500 dilution) or Alexa Fluor 568-conjugated anti-mouse secondary antibody (1:500 dilution) for 1 h at room temperature. F-actin in dHL60 cells was stained by using Alexa Fluor 568-conjugated phalloidin (1:100 dilution). Lipid membrane was stained with CM-DiI (1:200 dilution). Cells were visualized with an LSM510 Meta inverted confocal microscope (Carl Zeiss, Jena, Germany) with an argon/krypton laser and a Plan Apo 40× or 63× 1.3 numerical aperture oil immersion lens. Images were acquired and processed with ZEN2011 Image software (Carl Zeiss) and Adobe Photoshop (San Jose, CA).

Gel Filtration Chromatography—0.1 mg of WDR26 or WDR123–661 in 0.2 ml of gel filtration buffer (10 mM Tris-HCl (pH 7.4), 150 mM NaCl, 1 mM EDTA, 1 mM DTT) was applied to a pre-equilibrated Superdex 200 GL10/300 column (GE Healthcare) and resolved at a flow rate of 0.35 ml/min at 4 °C. 0.15-ml fractions were collected, and a 10-μl aliquot of each fraction was subjected to Western blotting analysis with anti-WDR26 antibody. The column was calibrated using the following gel filtration standards (Bio-Rad): thyroglobulin (670 kDa), γ-globulin (158 kDa), ovalbumin (44 kDa), myoglobin (17 kDa), and vitamin B_{12} (1.35 kDa).

PLCβ2 Assay—PLCβ2 assays were performed as described previously (23) except that 5 ng of PLCβ2 was used. To determine the effect of WDR26 and its mutants on $G\beta_1\gamma_2$-mediated PLCβ2 activation, they were preincubated with $G\beta_1\gamma_2$ (0.1 μM) for 30 min at room temperature followed by the addition of lipid vesicles containing 50 μM phosphatidylinositol 4,5-bisphosphate, 5000–8000 cpm/assay [^{3}H]phosphatidylinositol 4,5-bisphosphate, 200 μM phosphatidylethanolamine, and 5 ng/assay PLCβ2. The reaction was initiated by the addition of 100 nM free $CaCl_2$ and incubated at 30 °C for 10 min as described previously (23).

Measurement of Total Inositol Phosphate (IP) Turnover—G$\beta\gamma$-mediated PLCβ2 activation was determined in HEK293 cells as described previously (21). Briefly, 1 day post-transfection, cells were labeled for 48 h with *myo*-[^{3}H]inositol (2 μCi/ml) in inositol-free DMEM containing 1% dialyzed FBS. After serum starvation for 4 h, 10 mM LiCl was added to the cells to initiate IP accumulation for 40 min. Total IPs were separated by AG 1-X8 columns and expressed as percentage of total [^{3}H]inositol incorporated into the intact cells.

Statistical Analysis—Data were expressed as mean ± S.E. Statistical comparisons between two groups were analyzed by two-tailed Student's *t* test ($p < 0.05$ was considered significant).

RESULTS

WDR26 Forms a Complex with Gβγ and PLCβ2—We showed previously that WDR26 interacts with endogenous G$\beta\gamma$ in Jurkat T cells stimulated with SDF1α, which activates the chemokine receptor CXCR4 (16). Given that WDR26 is required for G$\beta\gamma$-mediated PLC activation in these cells, we asked whether PLCβ2 was co-precipitated with WDR26 and G$\beta\gamma$ in a complex. Immunoprecipitation analyses of FLAG-WDR26 from Jurkat T cells stably expressing this protein indicated that WDR26 associated with endogenous PLCβ2 in both stimulated and unstimulated cells (Fig. 1*A*, *left panel*). In contrast, as we showed previously, WDR26 only formed a complex with G$\beta\gamma$, but not $G\alpha_i$, in stimulated cells, and the interaction of WDR26 with G$\beta\gamma$ decreased over time with prolonged SDF1α stimulation (16). Pretreatment of cells with pertussis toxin to uncouple receptors from $G_{i/o}$ proteins abolished the interaction of WDR26 with G$\beta\gamma$ but had no effect on the interaction of WDR26 with PLCβ2 (Fig. 1*A*, *left panel*). These findings suggest that WDR26 is constitutively associated with PLCβ2.

To determine whether WDR26 directly binds PLCβ2, we performed binding assays *in vitro* using purified proteins. As shown in Fig. 1*B*, *upper panel*, FLAG-WDR26 bound PLCβ2 in a dose-dependent manner with a binding affinity of 0.906 ± 0.002 μM. Reciprocal pulldown of His-PLCβ2 also showed that PLCβ2 bound WDR26 in a dose-dependent manner with a binding affinity of 0.44 ± 0.13 μM (Fig. 1*B*, *lower panel*). The binding affinity of WDR26 with PLCβ2 is comparable with that with G$\beta\gamma$ (~0.5 μM) (16). Because G$\beta\gamma$ also binds PLCβ2 with a similar affinity (~1 μM) (22), this raises a question of whether WDR26, G$\beta\gamma$, and PLCβ2 can form a trimeric complex. To test this, we examined the binding of $G\beta_1\gamma_2$ (0.2 μM) to a constant

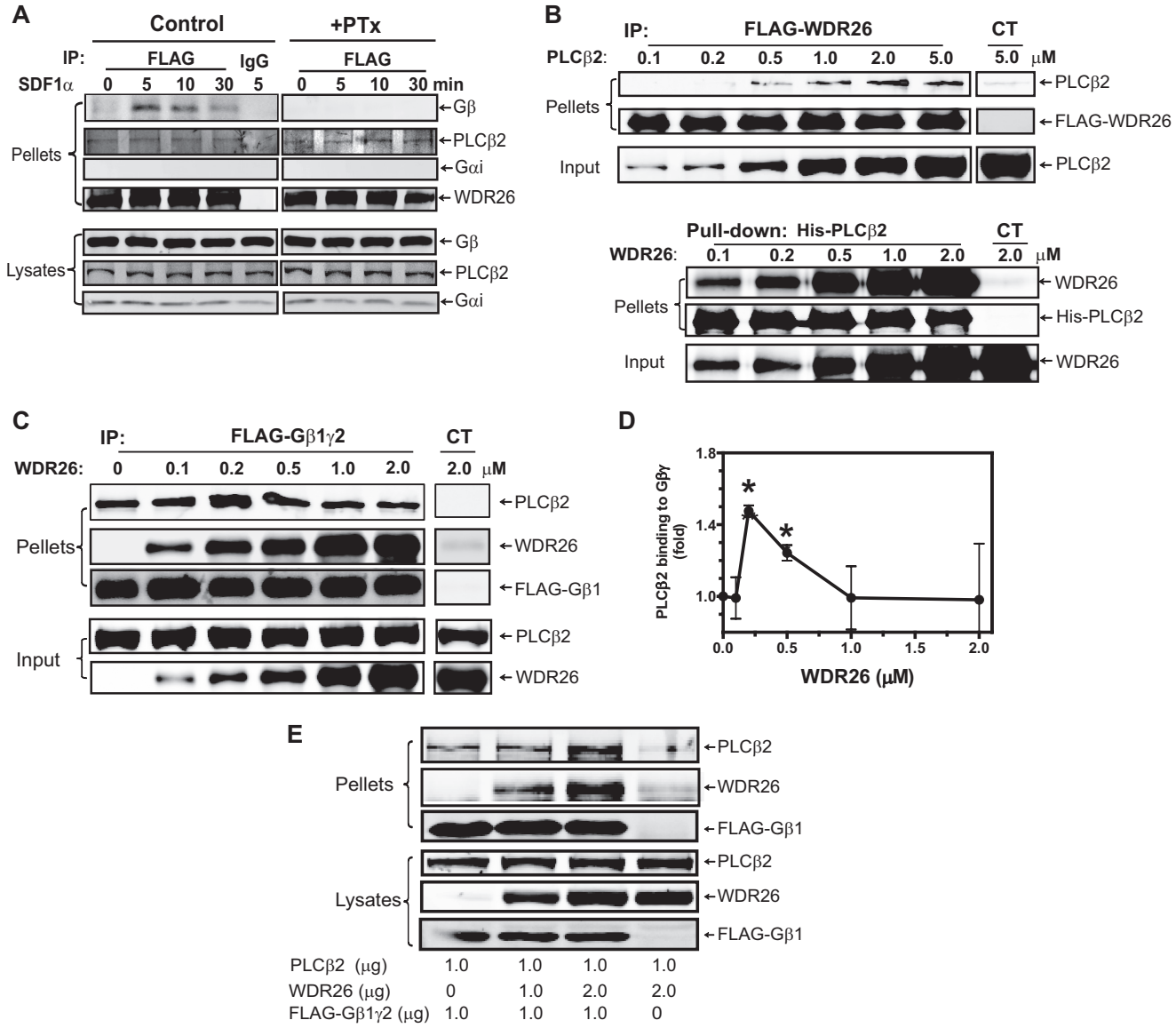

FIGURE 1. **WDR26 binds PLCβ2 and enhances its interaction with Gβγ.** *A*, co-immunoprecipitation of WDR26 with endogenous Gβγ and PLCβ2 from Jurkat T cells. FLAG-WDR26 was immunoprecipitated (*IP*) from Jurkat T cells pretreated with (+*PTx*) or without (*Control*) pertussis toxin overnight and stimulated with SDF1α (50 nM) for the indicated time using mouse IgG or an anti-FLAG antibody. The presence of Gβ, $G\alpha_i$, PLCβ2, and WDR26 in the immunoprecipitates (pellets) and lysates (2.5% of total) was detected with specific antibodies. *B*, direct interaction of WDR26 with PLCβ2 *in vitro*. *Upper panel*, FLAG-WDR26 (0.2 μM) was immunoprecipitated from Sf9 cell lysate by anti-FLAG antibody-conjugated beads and then incubated with increasing concentrations of purified PLCβ2. *Lower panel*, purified His-PLCβ2 (0.2 μM) was incubated with increasing concentrations of purified WDR26 and then precipitated with Ni-NTA beads as described under "Experimental Procedures." In the control (*CT*) samples, purified PLCβ2 or WDR26 alone was incubated with the beads. *C* and *D*, WDR26 enhanced Gβγ interaction with PLCβ2. Purified FLAG-$G\beta_1\gamma_2$ (0.2 μM) was incubated with PLCβ2 (0.5 μM) and increasing concentrations of WDR26 and then immunoprecipitated with control beads (*CT*) or anti-FLAG antibody-conjugated beads. Representative immunoblots are shown in *C*, and quantitative data from three independent experiments are shown in *D*. *, $p < 0.05$ indicates significance *versus* PLCβ2 binding to Gβγ in the absence of WDR26. *E*, WDR26 enhanced Gβγ interaction with PLCβ2 in intact cells. HEK293 cells were transfected with the indicated concentrations of FLAG-$G\beta_1\gamma_2$, PLCβ2, and WDR26. Cell lysates were immunoprecipitated with an anti-FLAG antibody. The presence of proteins in the immunoprecipitates (pellets) and lysates was determined by blotting for FLAG, WDR26, and PLCβ2. Unless indicated, representative blots from at least three independent experiments with similar results are shown for all figures. *Error bars* represent S.E.

amount of PLCβ2 (0.5 μM) in the presence of increasing concentrations of WDR26 (0–2 μM). As shown in Fig. 1*C*, WDR26 was co-precipitated with $G\beta_1\gamma_2$ and PLCβ2 in a complex. Moreover, the presence of WDR26 enhanced the binding of PLCβ2 to $G\beta_1\gamma_2$ in a dose-dependent manner. The enhanced binding peaked at 0.5 μM WDR26 and became less obvious at higher concentrations of WDR26. Similarly, co-expression with WDR26 also promoted Gβγ interaction with PLCβ2 in HEK293 cells (Fig. 1*E*). These findings indicate that at optimal concentrations WDR26 is able to form a complex containing both PLCβ2 and $G\beta_1\gamma_2$, thereby enhancing PLCβ2 interaction with $G\beta_1\gamma_2$. In contrast, excess WDR26 may bind to PLCβ2 and $G\beta_1\gamma_2$ individually and is therefore unable to increase the binding of PLCβ2 to $G\beta_1\gamma_2$.

WDR26 and PLCβ2 Bind to an Overlapping, but Not Identical, Site on $G\beta_1\gamma_2$—WDR26 binds to the Gα contact surface on $G\beta_1\gamma_2$, which is known to interact with diverse effectors including PLCβ2 (16). To understand the molecular basis for the abil-

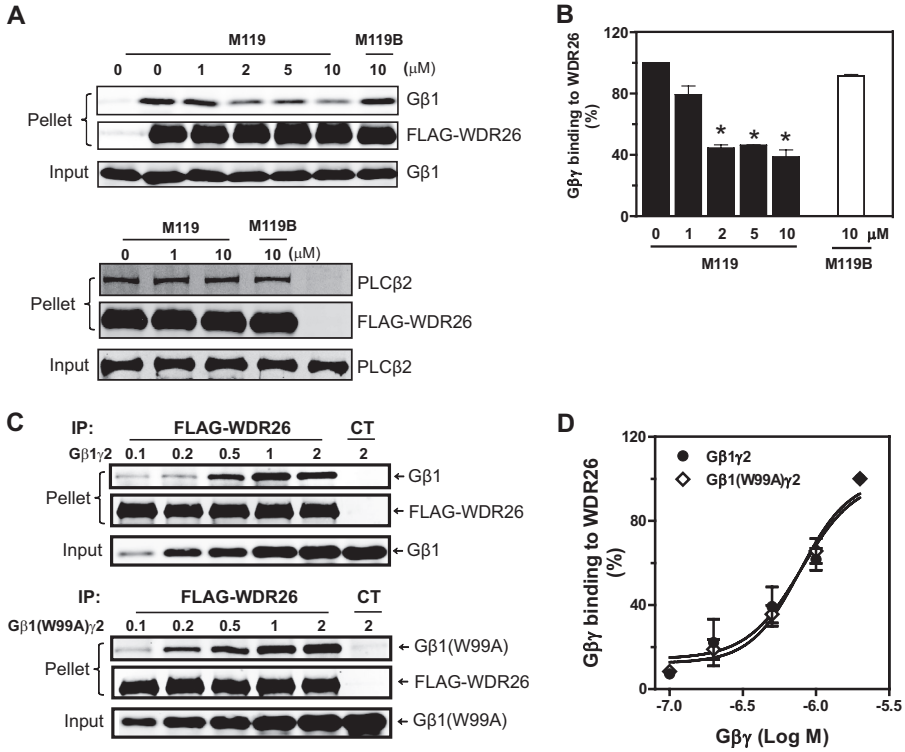

FIGURE 2. **The binding sites of WDR26 on $G\beta_1\gamma_2$.** *A* and *B*, purified FLAG-WDR26 (0.2 μM) was incubated with $G\beta_1\gamma_2$ (0.5 μM) (*upper panel*) or PLCβ2 (1 μM) (*lower panel*) in the presence or absence of the indicated concentrations of M119 and M119B and then immunoprecipitated (*IP*) with an anti-FLAG antibody. Representative immunoblots are shown in *A*, and quantitative data from at least three independent experiments are shown in *B*. *, $p < 0.05$ indicates significance *versus* binding in the absence of inhibitors. *C* and *D*, binding of FLAG-WDR26 to $G\beta_1\gamma_2$ and $G\beta_1$W99Aγ_2. Representative immunoblots are shown in *C*, and quantitative data from three independent experiments are shown in *D*. *Error bars* represent S.E. *CT*, control.

ity of WDR26 to form a complex with PLCβ2 and $G\beta_1\gamma_2$, we further characterized the binding sites of WDR26 on $G\beta_1\gamma_2$. Initially, we used small molecules, M119 and gallein, for competition binding assays because they bind to a "hot spot" on $G\beta_1\gamma_2$ that interacts with multiple effectors including PLCβ2 (24, 25). M119, but not its inactive analog, M119B, inhibited WDR26 binding to $G\beta_1\gamma_2$ at a concentration range that is known to inhibit PLCβ2 binding to $G\beta_1\gamma_2$ (Fig. 2*A*, *upper panel*, and *B*). Similar results were obtained with gallein (data not shown). In contrast, M119 had no effect on WDR26 interaction with PLCβ2 (Fig. 2*A*, *lower panel*), suggesting that M119 does not bind to WDR26. These data indicate that WDR26 and PLCβ2 share a common binding site on $G\beta_1\gamma_2$.

To further characterize specific residues on Gβγ required for binding WDR26 and PLCβ2, we evaluated WDR26 binding to a Gβγ mutant defective in binding to and activating PLCβ2, $G\beta_1$W99Aγ_2 (23, 26). The binding of WDR26 to $G\beta_1$W99Aγ_2 was comparable with that of the wild-type $G\beta_1\gamma_2$ (Fig. 2*B*), suggesting that Gβγ likely uses distinct residues within the hot spot for binding WDR26 and PLCβ2.

WDR26 Uses the Same Domains for Binding $G\beta_1\gamma_2$ and PLCβ2—We showed previously that the C-terminal fragment of WDR26 consisting of the LisH-CTLH and WD40 domains is involved in binding Gβγ (16). To identify the binding sites of PLCβ2 on WDR26, the interaction of PLCβ2 with a series of WDR26 deletion mutants was tested (Fig. 3). Most of the mutants can be readily detected in the immunoprecipitates, but only a small amount of WDR123–231 was detected in the precipitates (Fig. 3). This is probably due to its lower level of

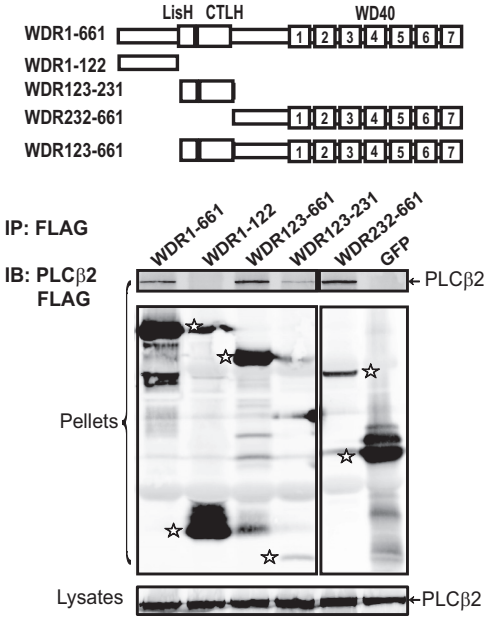

FIGURE 3. **The binding sites of PLCβ2 on WDR26.** HEK293 cells were transfected with PLCβ2 and FLAG-tagged GFP, full-length WDR26 (WDR1–661), or the indicated WDR26 deletion mutants. Cell lysates were immunoprecipitated (*IP*) with an anti-FLAG antibody as described in Fig. 1. The bands corresponding to GFP, WDR26, and its mutants in the immunoprecipitates (pellets) are indicated by *stars*. A schematic representation of the WDR26 structure and its mutants is shown in the *top panel*. *IB*, immunoblot.

expression or low efficiency of retention to the blotting membrane because of its small size (molecular mass, ~10 kDa). As compared with the full-length WDR26, mutants WDR123–

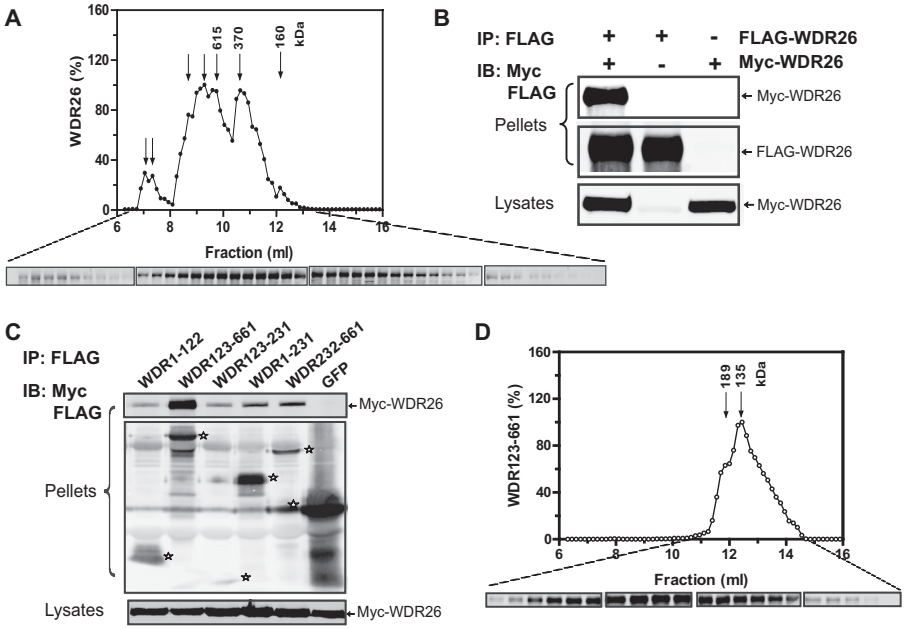

FIGURE 4. **Oligomerization of WDR26 and its mutant.** *A*, gel filtration analysis of purified WDR26 was performed as described under "Experimental Procedures." The elution profile of WDR26 was determined by Western blotting analysis of each fraction (0.15 ml). The molecular mass of each peak fraction calculated from standards (1.35–670 kDa) is indicated in the graph, and representative blots of each fraction are shown under the graph. *B*, formation of WDR26 oligomers *in vivo*. HEK293 cells were transfected with FLAG-WDR26 together with or without myc-WDR26. Cell lysates were subjected to immunoprecipitation (*IP*) with an anti-FLAG antibody. Representative blots are shown. *C*, interaction of WDR26 with its deletion mutants. Co-immunoprecipitation was performed in HEK293 cells transfected with the full-length myc-WDR26 and FLAG-tagged GFP or WDR26 mutants as described in *B*. The bands corresponding to GFP and WDR26 mutants in the precipitates are indicated by *stars*. *D*, gel filtration analysis of purified WDR123–661 mutant was performed as described in *A*. *IB*, immunoblot.

231, WDR123–661, and WDR232–661 retained the capacity to bind PLCβ2, whereas WDR1–122 failed to bind PLCβ2 (Fig. 3). These data indicate that the LisH-CTLH and WD40 domains of WDR26 are involved in binding PLCβ2. Interestingly, the WDR26 mutants that bound PLCβ2 also interact with Gβγ (16), suggesting that PLCβ2 and Gβγ may share overlapping binding sites on WDR26.

WDR26 Exists in Oligomers—Given that WDR26 and PLCβ2 share overlapping binding sites on Gβγ and that the same domains of WDR26 are involved in binding PLCβ2 and Gβγ, we were surprised to find they still formed a complex. Based on this observation, we questioned whether WDR26 forms a homodimer or a larger oligomer. Gel filtration analysis of purified WDR26 with a Superdex 200 column showed that WDR26 eluted in several fractions with peaks corresponding to ~160, 370, and larger than 600 kDa, the separation limit of the column (Fig. 4*A*). The fractions with peaks larger than 370 kDa appeared to be predominant (Fig. 4*A*). Given that the monomer of WDR26 is about 75 kDa, these results indicate that WDR26 exist in a mixture of multimers with higher order oligomers larger than a pentamer (~375 kDa) being predominant (>90%) (Fig. 4*A*). The formation of WDR26 oligomers was unlikely simply due to protein aggregation because they were still detected when gel filtration was performed with WDR26 tagged with the MBP, which enhances the solubility of fusion proteins (data not shown). To verify these findings in mammalian cells, we co-transfected FLAG- and myc-tagged WDR26 in HEK293 cells and then performed co-immunoprecipitation assays with anti-FLAG antibody. Myc-WDR26 was co-immunoprecipitated with FLAG-WDR26 (Fig. 4*B*), indicating that they formed oligomers.

To identify the structural elements required for WDR26 oligomerization, we evaluated the interaction of WDR26 deletion mutants with the full-length WDR26. The N-terminal fragment WDR1–122 did not bind WDR26, but the C-terminal fragment WDR123–661 retained the same binding to WDR26 as the full-length WDR26. Deletion of either the LisH-CTLH domain (WDR232–661) or WD40 domain (WDR123–231 and WDR1–231) from WDR123–661 impaired its binding to WDR26, indicating that both domains are involved in WDR26 oligomerization (Fig. 4*C*). Interestingly, gel filtration analysis of purified WDR123–661 showed that unlike the full-length WDR26, which formed predominantly larger oligomers, it existed primarily in a dimer (~135 kDa) or trimer (~189 kDa) (Fig. 4*D*). These findings suggest that the N-terminal fragment WDR1–122 is required for stabilization of WDR26 in the form of higher order oligomers.

WDR26 Enhances Gβγ-mediated PLCβ2 Activation—To determine whether the ternary complex formed by WDR26, Gβγ, and PLCβ2 is signaling-competent, we tested Gβγ-stimulated PLCβ2 activity in the presence of increasing concentrations of WDR26. WDR26 did not alter the basal activity of PLCβ2 but increased Gβγ-stimulated PLCβ2 activity with a bell-shaped curve (Fig. 5*A*). The concentrations of WDR26 required for enhancing PLCβ2 activity were consistent with those required for increasing PLCβ2 binding to Gβγ (Fig. 1, *C* and *D*), indicating that WDR26 enhanced PLCβ2 activation primarily through promoting PLCβ2 interaction with Gβγ. In support of this notion, we found that WDR26 was unable to rescue PLCβ2 activation by $G\beta_1W99A\gamma_2$, which is deficient in binding PLCβ2 (Fig. 5*B*). Additionally, the WDR123–661 mutant inhibited the interaction between $G\beta_1\gamma_2$ and PLCβ2

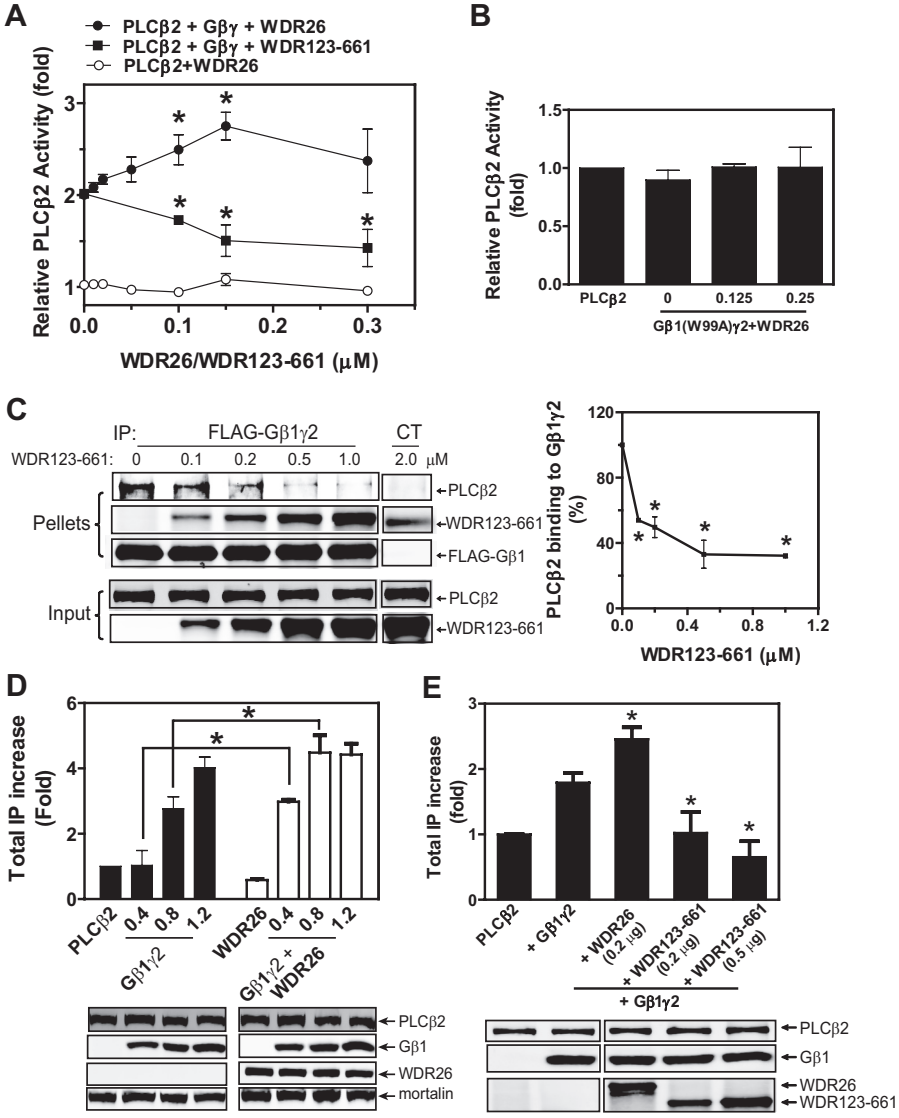

FIGURE 5. **The effect of WDR26 and WDR123–661 on Gβγ-mediated PLCβ2 activation.** *A*, the effect of purified WDR26 or WDR123–661 on the basal activity of PLCβ2 (○) or $G\beta_1\gamma_2$-stimulated PLCβ2 (● and ■, respectively) was determined as described under "Experimental Procedures." Data are expressed as -fold increases of PLCβ2 activity over its basal activity. *, $p < 0.05$ indicates significance *versus* $G\beta_1\gamma_2$-stimulated PLCβ2 activity in the absence of WDR26 or WDR123–661. *B*, WDR26 could not rescue the deficiency of $G\beta_1$W99Aγ_2 in stimulating PLC*β2 in vitro*. The effect of the indicated concentrations of WDR26 (μM) on $G\beta_1$W99Aγ_2 (0.1 μM)-mediated PLCβ2 stimulation was determined as described in *A*. *C*, WDR123–661 inhibited PLCβ2 interaction with $G\beta_1\gamma_2$. The effect of purified WDR123–661 on PLCβ2 interaction with $G\beta_1\gamma_2$ was determined *in vitro* as described in Fig. 1. Representative images are shown in the *left panel*. Quantitative data shown in the *right panel* are expressed as percentage of PLCβ2 binding to $G\beta_1\gamma_2$ in the absence of WDR123–661. *, $p < 0.05$ indicates significance *versus* PLCβ2 binding to $G\beta_1\gamma_2$ in the absence of WDR123–661. *D*, WDR26 enhances $G\beta_1\gamma_2$-stimulated PLCβ2 activity *in vivo*. Total IPs were quantified in HEK293 cells transfected with PLCβ2 alone (PLCβ2; 0.1 μg), PLCβ2 together with WDR26 (0.2 μg) (WDR26), or the indicated concentration of $G\beta_1\gamma_2$ (*Gβ1γ2*) (0.4, 0.8 and 1.2 μg) or $G\beta_1\gamma_2$ plus WDR26 (*Gβ1γ2+WDR26*). Data are expressed as -fold increases of total IP over that produced by PLCβ2 alone after subtraction of basal IP accumulation in mock transfected cells. Representative blots of protein expression are shown under the graph. *, $p < 0.05$ indicates significance ($n = 3$). *E*, WDR123–661 inhibited $G\beta_1\gamma_2$-stimulated PLCβ2 activity *in vivo*. Total IPs were quantified in HEK293 cells transfected with PLCβ2 alone (*PLCβ2*; 0.1 μg), PLCβ2 together with $G\beta_1\gamma_2$ (0.8 μg) (+*Gβ1γ2*), or $G\beta_1\gamma_2$ (0.8 μg) plus the indicated concentration of WDR26 or WDR123–661 as described in *B*. Representative blots of protein expression are shown under the graph. *, $p < 0.05$ indicates significance *versus* total IPs generated by $G\beta_1\gamma_2$-stimulated PLCβ2 ($n = 3$). *Error bars* represent S.E. *IP*, immunoprecipitation.

and consequently blocked $G\beta_1\gamma_2$-mediated PLCβ2 activation in a dose-dependent manner (Fig. 5, *A* and *C*).

To verify the findings in intact cells, we co-transfected WDR26 with PLCβ2 and different concentrations of $G\beta_1\gamma_2$ in HEK293 cells and then analyzed IP accumulation. Gβγ alone was able to activate PLCβ2 in a dose-dependent manner (Fig. 5*D*). Co-transfection with WDR26 significantly enhanced the potency of $G\beta_1\gamma_2$ in activating PLCβ2, particularly with lower concentrations of $G\beta_1\gamma_2$ (0.4 and 0.8 μg) (Fig. 5*D*). WDR26 alone did not affect the basal activity of PLCβ2, nor did it affect the expression of PLCβ2 and $G\beta_1\gamma_2$ (Fig. 5*D*). In contrast, co-transfection with WDR123–661 inhibited $G\beta_1\gamma_2$-mediated PLCβ2 activation (Fig. 5*E*). Together, these findings indicate that WDR26 enhanced PLCβ2 activation by $G\beta_1\gamma_2$ both *in vitro* and in intact cells.

WDR26 Promotes PLCβ2 Membrane Translocation—We showed previously that stimulation of Jurkat T and dHL60 cells with chemoattractants leads to WDR26 translocation from the cytosol to the plasma membrane (16). Immunostaining analysis showed that in unstimulated dHL60 cells the cellular localiza-

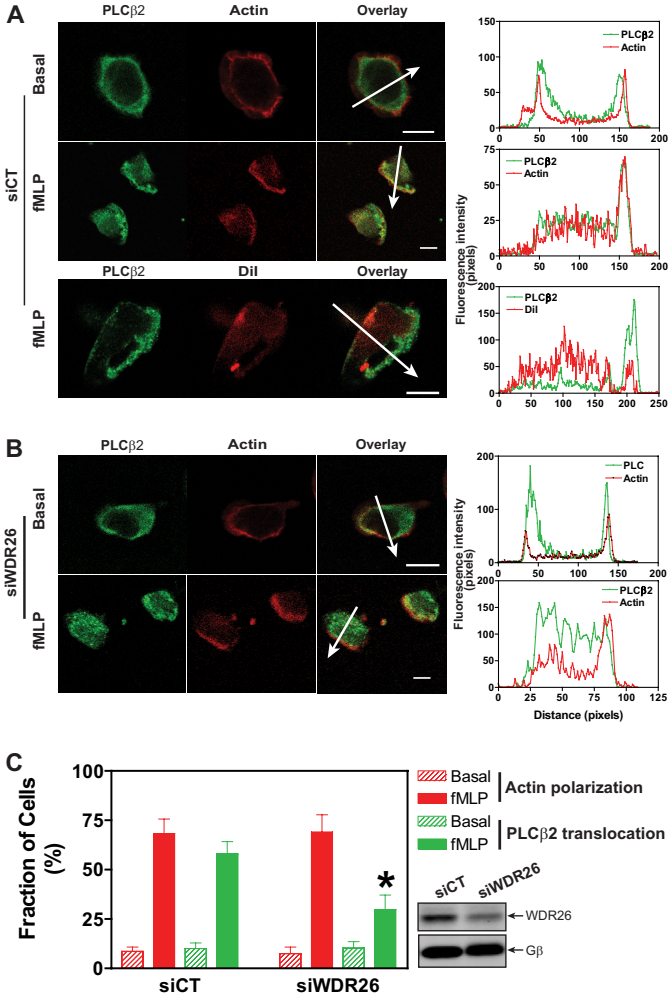

FIGURE 6. **WDR26 regulates PLCβ2 translocation.** dHL60 cells were transiently transfected with a control (*siCT*) (*A*) or WDR26 siRNA (*siWDR26*) (*B*) and stimulated with buffer (*Basal*) or fMLP (0.2 μM) for 2 min. After fixation and permeabilization, cells were stained with a rabbit anti-PLCβ2 antibody and Alexa Fluor 568-conjugated phalloidin or CM-DiI. Representative images are shown in *A* and *B*, and quantitative data from over 100 cells in three separate experiments are shown in *C*. *, $p < 0.05$ *versus* siCT. The graphs in the *right panel* show the distribution of fluorescence intensity of PLCβ2 and F-actin or CM-DiI along the *arrows* drawn across the cells. *Bar*, 10 μm. The level of WDR26 and Gβ expression in control and WDR26 siRNA cells is shown in representative blots in *C*. *Error bars* represent S.E.

tion of both WDR26 (16) and PLCβ2 was difficult to be determined by first glance as these cells have a large nucleus and a small fraction of cytosol. However, colocalization analysis of WDR26 and PLCβ2 with the cortical actin showed that they were located within the cortical actin, indicating that they were predominantly localized in the cytosol (Fig. 6*A*) (16). The cytosolic localization of WDR26 and PLCβ2 was confirmed by cell fractionation analysis (data not shown). Upon stimulation with fMLP, dHL60 cells became polarized, generating an F-actin-enriched lamellipodial membrane protrusion (Fig. 6*A*). As with WDR26 (16), PLCβ2 accumulated within the membrane protrusion (Fig. 6*A*). This accumulation was not an artifact of the increase in plasma membrane surface at the cell's protrusion because polarized cells labeled with the lipid membrane probe CM-DiI exhibited uniform CM-DiI fluorescence across the cell (Fig. 6*A*). Given that WDR26 bound PLCβ2, we asked whether WDR26 is required for PLCβ2 translocation to the membrane protrusion. Transient transfection of dHL60 cells with an siRNA against WDR26 led to about 50–60% reduction in the level of WDR26 expression (Fig. 6*C*). The down-regulation of WDR26 did not affect the response of dHL60 to fMLP-stimulated F-actin polarization, nor did it affect the cytosolic localization of PLCβ2 in unstimulated cells (Fig. 6, *B* and *C*). However, PLCβ2 translocation to the membrane protrusion was significantly inhibited in fMLP-stimulated dHL60 cells (Fig. 6, *B* and *C*). These findings indicate that WDR26 regulates the membrane translocation of PLCβ2.

We showed previously that down-regulation of WDR26 in dHL60 cells abolished fMLP-stimulated Ca^{2+} signaling, which is known to be mediated by PLCβ2/3 (16). To determine whether WDR26-regulated PLCβ2 translocation contributed to PLCβ2 activity, we first tested whether membrane translocation alone is sufficient for PLCβ2 activation. To render PLCβ2 membrane localization, we attached a myristoylation sequence to its N terminus. We then transfected different concentration of the wild-type PLCβ2 and myr-PLCβ2 in HEK293 cells and compared their basal activities in generating total IP. As expected, confocal microcopy analysis indicated that PLCβ2 was expressed in the cytosol, whereas myr-PLCβ2 was located primarily in the plasma membranes (Fig. 7*A*). Overexpression of either the wild-type or myr-PLCβ2 caused an expression level-dependent increase in IP accumulation ($r^2 = 0.84$ and 0.71 for the wild-type and myr-PLCβ2, respectively, $p < 0.01$) (Fig. 7*E*). At a similar expression level, myr-PLCβ2 displayed a higher activity in mediating IP production than its wild-type counterpart (Fig. 7*E*). Based on the slope of their dose-response curves, the basal activity of myr-PLCβ2 is estimated to be ~2-fold higher than that of the wild-type PLCβ2 (0.212 ± 0.077 *versus* 0.083 ± 0.025, $p < 0.05$, $n = 3$). Notably, co-transfection of myr-PLCβ2 with $G\beta_1\gamma_2$ caused a further increase in IP production (Fig. 7*F*), suggesting that membrane translocation alone is insufficient for maximum activation of PLCβ2.

To provide evidence that WDR26-mediated PLCβ2 translocation contributes to its activation, we generated myr-WDR26 and co-expressed it with PLCβ2. As expected, the wild-type WDR26 alone was expressed primarily in the cytosol, whereas myr-WDR26 was expressed in the plasma membrane (Fig. 7*B*). Co-expression of myr-WDR26 but not the wild-type WDR26 with PLCβ2 resulted in a significant amount of PLCβ2 localized in the plasma membrane (Fig. 7*C*). Corresponding to their membrane localization, co-expression with the wild-type WDR26 had no effects on the basal activity of PLCβ2, whereas co-expression with myr-WDR26 led to PLCβ2 activity (Fig. 7*G*).

DISCUSSION

In this study, we have demonstrated that the Gβγ-binding protein WDR26 serves as a scaffolding protein to promote Gβγ-mediated PLCβ2 activation by regulating PLCβ2 membrane translocation and interaction with Gβγ. PLCβ2 is a cytosolic protein (12, 27). To hydrolyze its membrane-localized substrate, phosphatidylinositol 4,5-bisphosphate, PLCβ2 must first be translocated to the membrane. Indeed, agonist-stimulated PLCβ2 translocation has been demonstrated in both neu-

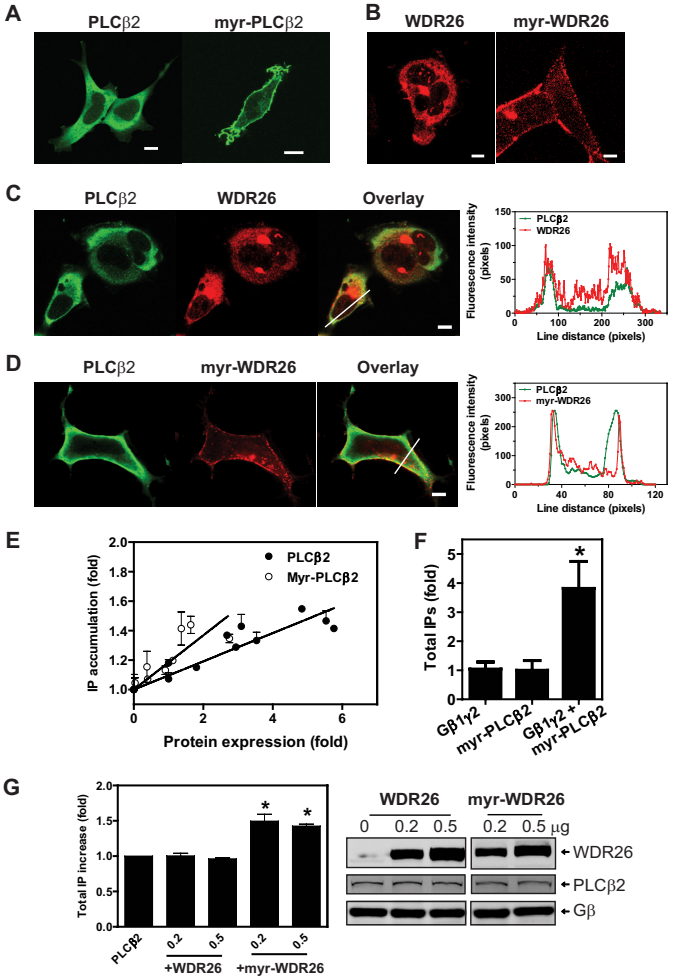

FIGURE 7. **Membrane translocation of PLCβ2 and WDR26 regulates PLCβ2 activity.** *A–D*, cellular localization of PLCβ2 (*A*, *C*, and *D*), myr-PLCβ2 (*A*), FLAG-WDR26 (*B* and *C*), and myr-FLAG-WDR26 (*B* and *D*). HEK293 cells were transiently transfected with the indicated constructs and stained with a rabbit anti-PLCβ2 and/or mouse anti-FLAG. Representative images are shown. The graphs in the *right panel* of *C* and *D* show the distribution of fluorescence intensity of PLCβ2 and WDR26 along the *lines* drawn across the cells. *Bar*, 5 μm. *E*, total IPs in HEK293 cells transfected with increasing concentrations of PLCβ2 or myr-PLCβ2. The levels of protein expression were quantified by Western blotting and expressed as -fold increases over that in cells transfected with the smallest amount of plasmids. IP accumulation is expressed as -fold increases over that in cells expressing the lowest level of proteins ($n = 3$). *F*, total IP accumulation in HEK293 cells transfected with $G\beta_1\gamma_2$ (0.4 μg), myr-PLCβ2 (0.2 μg), or $G\beta_1\gamma_2$ (0.4 μg) plus myr-PLCβ2 (0.2 μg). Data are expressed as -fold increases of IPs over that generated by cells expressing myr-PLCβ2 alone. *, $p < 0.05$ indicates significance *versus* myr-PLCβ2 alone ($n = 4$). *G*, total IP accumulation in HEK293 cells transfected with PLCβ2 (0.1 μg) alone or PLCβ2 together with the indicated concentration (μg) of WDR26 or myr-WDR26. Data are expressed as -fold increases of IPs over that generated by cells expressing PLCβ2 alone. *, $p < 0.05$ indicates significance *versus* PLCβ2 alone ($n = 3$). Representative images in the *right panel* show the level of protein expression. *Error bars* represent S.E.

trophils and macrophages (12, 28). However, the underlying mechanisms for PLCβ2 translocation have not yet been defined. Although PLCβ2 directly binds Gβγ, which is localized in the membrane, it is not clear whether interaction with Gβγ itself is sufficient for translocation. Our data indicate that PLCβ2 membrane translocation critically depends on its interaction with WDR26. As with Gβγ, PLCβ2 directly binds WDR26. However, unlike Gβγ, PLCβ2 binding to WDR26 does not require the activation of G protein-coupled receptors, suggesting that WDR26 and PLCβ2 likely exist in a preformed complex in the cytosol of unstimulated cells. In support of this notion, both endogenous WDR26 and PLCβ2 are predominantly located in the cytosol of unstimulated dHL60 cells. Moreover, they are both translocated to the membrane protrusion by stimulation with the chemoattractant fMLP. The role of WDR26 in facilitating PLCβ2 membrane translocation is further demonstrated by the findings that partially suppressing WDR26 in dHL60 cells inhibited PLCβ2 translocation but had no significant effects on actin polymerization and cell polarization, suggesting that PLCβ2 translocation is not simply the result of cell polarization but rather its interaction with WDR26. In line with these findings, co-expressing PLCβ2 with the membrane-localized WDR26 in HEK293 cells results in a significant enhancement of PLCβ2 membrane localization. It is not clear from our studies how WDR26 translocation is regulated. Our previous work suggests that WDR26 is not simply anchored to the membrane protrusion by its interaction with Gβγ because the concentration gradient of WDR26 from the leading to trailing edge in a polarized leukocyte is significantly steeper than that of Gβγ (16). However, WDR26 translocation is sensitive to pertussis toxin treatment, suggesting that activated $G\alpha_{i/o}$ or Gβγ signaling is required for the translocation (16).

Membrane translocation has been shown to be sufficient to cause activation of a number of enzymes including the Gβγ effector PI3Kγ (11). It is not yet clear whether membrane translocation is sufficient for PLCβ2 activation. Recent studies of Rac-dependent activation of PLCβ2 have suggested that Rac1 may activate PLCβ2 by inducing membrane translocation because there is no significant conformational difference between the structures of free and Rac1-bound PLCβ2 (29). Our findings that targeting PLCβ2 to the membrane either by attaching a myristoylation sequence to its N terminus or by co-expression with myristoylated WDR26 enhances its basal activity to hydrolyze phosphatidylinositol 4,5-bisphosphate have provided direct evidence to support the role of membrane translocation in PLCβ2 activation. However, it remains unclear how membrane localization causes PLCβ2 activation. Previous work by Sondek and co-workers (30) has identified a linker region between the X and Y domains of the PLCβ2 catalytic domain that is folded back to occlude its catalytic site. This inhibitory linker consists of a high density of negatively charged residues and was proposed to autoinhibit PLCβ2. Upon PLCβ2 recruitment to negatively charged substrate membranes, the inhibitory linker is displaced from the active site by electrostatic repellence, leading to PLCβ2 activation. This hypothesis was supported by the findings that deletion of the linker region is sufficient to cause PLCβ2 activation in the absence of any stimuli (30). However, the PLCβ2 mutant with the linker deletion exhibited up to a 20-fold increase in basal activity, which is significantly larger than what we observed with the membrane-targeted PLCβ2 (~2-fold). Although the observed different activities of the PLCβ2 deletion mutant and membrane-targeted PLCβ2 could be due to different assay conditions used by the two laboratories, these findings may also suggest that the increased PLCβ2 activity by translocation cannot be simply attributed to the displacement of the inhibitory linker.

Although membrane translocation is likely the first step of PLCβ2 activation *in vivo*, it has been shown previously that Gβγ can activate PLCβ2 independently of its translocation *in vitro* (14, 15). These findings indicate that once arriving at the membrane PLCβ2 is further activated by direct interaction with Gβγ. Interestingly, under such a condition, Gβγ-mediated PLCβ2 activation can be further enhanced by WDR26. The effect of WDR26 on PLCβ2 activation is concentration-dependent and correlated to its ability to enhance Gβγ interaction with PLCβ2. Given that WDR26 interacts with both Gβγ and PLCβ2, these findings indicate that at optimal concentrations WDR26 forms a complex with Gβγ and PLCβ2 that promotes Gβγ-mediated PLCβ2 activation. Intriguingly, the binding sites of WDR26 on Gβγ appear to involve a contact surface on Gβγ that is required for binding and activation of many effectors including PLCβ2. Moreover, the binding of Gβγ and PLCβ2 to WDR26 involves similar domains of WDR26. These findings raise the question of how WDR26, Gβγ, and PLCβ2 can be assembled into a complex. Previous work has found that Gβγ contains multiple binding sites for PLCβ2. In addition to the Gα contact surface, the N-terminal coiled coil domain and the outer surface of the Gβ are also involved in binding PLCβ2 (22, 31). In the absence of other constraints, Gβγ activates PLCβ2 primarily through the $G\alpha_t$ contact region (26). However, in the presence of one Gβγ-interacting protein, AGS8, Gβγ binds to PLCβ2 through an alternative site located at the N terminus of Gβ (23). Consequently, AGS8, Gβγ, and PLCβ2 can co-exist in a complex. Moreover, AGS8 rescues PLCβ2 binding and activation by an inactive Gβ that contains a mutation ($G\beta_1$W99A) in the effector contact surface. Our data indicate that WDR26 may not use the same mechanism to form a complex with Gβγ and PLCβ2 because unlike AGS8, which only binds Gβγ, WDR26 interacts with both Gβγ and PLCβ2. Moreover, WDR26 was unable to restore the ability of $G\beta_1$W99Aγ_2 to activate PLCβ2, suggesting that unlike AGS8 WDR26 does not direct Gβγ to use the alternative site for binding and activation of PLCβ2. Rather, our findings that WDR26 exists in oligomers suggest that WDR26 may use different monomers to bind Gβγ and PLCβ2, thereby bringing Gβγ and PLCβ2 in close proximity for enhanced interaction and activation. In this sense, WDR26 serves as a scaffolding protein to assemble Gβγ and PLCβ2 in a complex.

The interactions of WDR26 with Gβγ and PLCβ2 are likely to be transient in cells because we cannot isolate WDR26, Gβγ, and PLCβ2 as a stable complex by gel filtration chromatography, nor can we accurately determine the stoichiometric relationship of their bindings by binding assays involving extensive washing steps (data not shown). Interestingly, the ability of WDR26 to enhance Gβγ and PLCβ2 interaction and activation appears to depend on its formation of oligomers larger than a pentamer because the N-terminal truncation mutant of WDR26, WDR123–661, which predominantly exists in dimers and trimers, fails to promote PLCβ2 binding and activation by Gβγ. Rather, WDR123–661 exhibits a dominant negative activity of inhibiting Gβγ and PLCβ2 interaction and activation both *in vitro* and *in vivo*.

In summary, our studies have uncovered a novel mechanism of regulating Gβγ signaling by a WD40 repeat protein that serves as a scaffolding protein to promote the interaction and activation of PLCβ2 by Gβγ. Our data suggest that in unstimulated cells WDR26 forms a complex with PLCβ2 in the cytosol. Upon G protein-coupled receptor-mediated G protein activation, WDR26 facilitates the recruitment of PLCβ2 to the plasma membrane. Once on the membrane, WDR26 binds to Gβγ, thereby bringing PLCβ2 in close proximity to Gβγ for interaction and activation. Given that WDR26 is ubiquitously expressed and is required for the efficient activation of other Gβγ effectors such as PI3Kγ (16), such a mechanism of regulation by WDR26 may extend beyond PLCβ2 (32). In addition to PLCβ2, Gβγ can also stimulate PLCβ3. Although the expression of PLCβ2 is limited to leukocytes, PLCβ3 is ubiquitously expressed. It will be interesting to determine whether WDR26 can also bind PLCβ3 and regulate Gβγ-mediated PLCβ3 activation in other cell types. Moreover, our previous work has already demonstrated that the regulation of Gβγ signaling by WDR26 is critical for leukocyte migration (16). Recent work has shown that Gβγ signaling is also involved in numerous pathological conditions such as heart failure and tumor growth and metastasis (5, 33). It would be interesting to determine whether aberrant regulation of Gβγ signaling by WDR26 contributes to these pathological conditions.

Acknowledgment—We greatly appreciated Caitlin Runne for proofreading the manuscript.

REFERENCES

1. Oldham, W. M., and Hamm, H. E. (2008) Heterotrimeric G protein activation by G-protein-coupled receptors. *Nat. Rev. Mol. Cell Biol.* **9,** 60–71
2. Smrcka, A. V. (2008) G protein βγ subunits: central mediators of G protein-coupled receptor signaling. *Cell. Mol. Life Sci.* **65,** 2191–2214
3. Chen, S., Lin, F., Shin, M. E., Wang, F., Shen, L., and Hamm, H. E. (2008) RACK1 regulates directional cell migration by acting on Gβγ at the interface with its effectors PLCβ and PI3Kγ. *Mol. Biol. Cell* **19,** 3909–3922
4. Rickert, P., Weiner, O. D., Wang, F., Bourne, H. R., and Servant, G. (2000) Leukocytes navigate by compass: roles of PI3Kγ and its lipid products. *Trends Cell Biol.* **10,** 466–473
5. Tang, X., Sun, Z., Runne, C., Madsen, J., Domann, F., Henry, M., Lin, F., and Chen, S. (2011) A critical role of Gβγ in tumorigenesis and metastasis of breast cancer. *J. Biol. Chem.* **286,** 13244–13254
6. Whiteway, M. S., Wu, C., Leeuw, T., Clark, K., Fourest-Lieuvin, A., Thomas, D. Y., and Leberer, E. (1995) Association of the yeast pheromone response G protein βγ subunits with the MAP kinase scaffold Ste5p. *Science* **269,** 1572–1575
7. Gehrmann, J., Meister, M., Maguire, C. T., Martins, D. C., Hammer, P. E., Neer, E. J., Berul, C. I., and Mende, U. (2002) Impaired parasympathetic heart rate control in mice with a reduction of functional G protein βγ-subunits. *Am. J. Physiol. Heart Circ. Physiol.* **282,** H445–H456
8. Mirshahi, T., Jin, T., and Logothetis, D. E. (2003) Gβγ and KACh: old story, new insights. *Sci. STKE* **2003,** PE32
9. Tedford, H. W., and Zamponi, G. W. (2006) Direct G protein modulation of Cav2 calcium channels. *Pharmacol. Rev.* **58,** 837–862
10. Pitcher, J. A., Touhara, K., Payne, E. S., and Lefkowitz, R. J. (1995) Pleckstrin homology domain-mediated membrane association and activation of the β-adrenergic receptor kinase requires coordinate interaction with Gβγ subunits and lipid. *J. Biol. Chem.* **270,** 11707–11710
11. Brock, C., Schaefer, M., Reusch, H. P., Czupalla, C., Michalke, M., Spicher, K., Schultz, G., and Nürnberg, B. (2003) Roles of Gβγ in membrane recruitment and activation of p110γ/p101 phosphoinositide 3-kinase γ. *J. Cell Biol.* **160,** 89–99
12. Chiou, W. F., Tsai, H. R., Yang, L. M., and Tsai, W. J. (2004) C5a differen-

tially stimulates the ERK1/2 and p38 MAPK phosphorylation through independent signaling pathways to induced chemotactic migration in RAW264.7 macrophages. *Int. Immunopharmacol.* **4,** 1329–1341
13. Drin, G., and Scarlata, S. (2007) Stimulation of phospholipase Cβ by membrane interactions, interdomain movement, and G protein binding—how many ways can you activate an enzyme? *Cell. Signal.* **19,** 1383–1392
14. Romoser, V., Ball, R., and Smrcka, A. V. (1996) Phospholipase C β2 association with phospholipid interfaces assessed by fluorescence resonance energy transfer. G protein βγ subunit-mediated translocation is not required for enzyme activation. *J. Biol. Chem.* **271,** 25071–25078
15. Runnels, L. W., Jenco, J., Morris, A., and Scarlata, S. (1996) Membrane binding of phospholipases C-β1 and C-β2 is independent of phosphatidylinositol 4,5-bisphosphate and the alpha and beta gamma subunits of G proteins. *Biochemistry* **35,** 16824–16832
16. Sun, Z., Tang, X., Lin, F., and Chen, S. (2011) The WD40 repeat protein WDR26 binds Gβγ and promotes Gβγ-dependent signal transduction and leukocyte migration. *J. Biol. Chem.* **286,** 43902–43912
17. Zhao, J., Liu, Y., Wei, X., Yuan, C., Yuan, X., and Xiao, X. (2009) A novel WD-40 repeat protein WDR26 suppresses H_2O_2-induced cell death in neural cells. *Neurosci. Lett.* **460,** 66–71
18. Zhu, Y., Wang, Y., Xia, C., Li, D., Li, Y., Zeng, W., Yuan, W., Liu, H., Zhu, C., Wu, X., and Liu, M. (2004) WDR26: a novel Gβ-like protein, suppresses MAPK signaling pathway. *J. Cell. Biochem.* **93,** 579–587
19. Feng, Y., Zhang, C., Luo, Q., Wei, X., Jiang, B., Zhu, H., Zhang, L., Jiang, L., Liu, M., and Xiao, X. (2012) A novel WD-repeat protein, WDR26, inhibits apoptosis of cardiomyocytes induced by oxidative stress. *Free Radic. Res.* **46,** 777–784
20. Wei, X., Song, L., Jiang, L., Wang, G., Luo, X., Zhang, B., and Xiao, X. (2010) Overexpression of MIP2, a novel WD-repeat protein, promotes proliferation of H9c2 cells. *Biochem. Biophys. Res. Commun.* **393,** 860–863
21. Chen, S., Dell, E. J., Lin, F., Sai, J., and Hamm, H. E. (2004) RACK1 regulates specific functions of Gβγ. *J. Biol. Chem.* **279,** 17861–17868
22. Chen, S., Lin, F., and Hamm, H. E. (2005) RACK1 binds to a signal transfer region of Gβγ and inhibits phospholipase C β2 activation. *J. Biol. Chem.* **280,** 33445–33452
23. Yuan, C., Sato, M., Lanier, S. M., and Smrcka, A. V. (2007) Signaling by a non-dissociated complex of G protein βγ and α subunits stimulated by a receptor-independent activator of G protein signaling, AGS8. *J. Biol. Chem.* **282,** 19938–19947
24. Bonacci, T. M., Mathews, J. L., Yuan, C., Lehmann, D. M., Malik, S., Wu, D., Font, J. L., Bidlack, J. M., and Smrcka, A. V. (2006) Differential targeting of Gβγ-subunit signaling with small molecules. *Science* **312,** 443–446
25. Lehmann, D. M., Seneviratne, A. M., and Smrcka, A. V. (2008) Small molecule disruption of G protein βγ subunit signaling inhibits neutrophil chemotaxis and inflammation. *Mol. Pharmacol.* **73,** 410–418
26. Ford, C. E., Skiba, N. P., Bae, H., Daaka, Y., Reuveny, E., Shekter, L. R., Rosal, R., Weng, G., Yang, C. S., Iyengar, R., Miller, R. J., Jan, L. Y., Lefkowitz, R. J., and Hamm, H. E. (1998) Molecular basis for interactions of G protein βγ subunits with effectors. *Science* **280,** 1271–1274
27. Smrcka, A. V., and Sternweis, P. C. (1993) Regulation of purified subtypes of phosphatidylinositol-specific phospholipase C β by G protein α and βγ subunits. *J. Biol. Chem.* **268,** 9667–9674
28. Tang, W., Zhang, Y., Xu, W., Harden, T. K., Sondek, J., Sun, L., Li, L., and Wu, D. (2011) A PLCβ/PI3Kγ-GSK3 signaling pathway regulates cofilin phosphatase slingshot2 and neutrophil polarization and chemotaxis. *Dev. Cell* **21,** 1038–1050
29. Jezyk, M. R., Snyder, J. T., Gershberg, S., Worthylake, D. K., Harden, T. K., and Sondek, J. (2006) Crystal structure of Rac1 bound to its effector phospholipase C-β2. *Nat. Struct. Mol. Biol.* **13,** 1135–1140
30. Hicks, S. N., Jezyk, M. R., Gershburg, S., Seifert, J. P., Harden, T. K., and Sondek, J. (2008) General and versatile autoinhibition of PLC isozymes. *Mol. Cell* **31,** 383–394
31. Yoshikawa, D. M., Bresciano, K., Hatwar, M., and Smrcka, A. V. (2001) Characterization of a phospholipase C β2-binding site near the amino-terminal coiled-coil of G protein βγ subunits. *J. Biol. Chem.* **276,** 11246–11251
32. Runne, C., and Chen, S. (2013) WD40-repeat proteins control the flow of Gβγ signaling for directional cell migration. *Cell Adh. Migr.* **7,** 214–218
33. Casey, L. M., Pistner, A. R., Belmonte, S. L., Migdalovich, D., Stolpnik, O., Nwakanma, F. E., Vorobiof, G., Dunaevsky, O., Matavel, A., Lopes, C. M., Smrcka, A. V., and Blaxall, B. C. (2010) Small molecule disruption of Gβγ signaling inhibits the progression of heart failure. *Circ. Res.* **107,** 532–539